Study of new flow field geometries to enhance water redistribution and pressure head losses reduction within PEM fuel cell

Kush Chadha, Serguei Martemianov, Anthony Thomas

Study of new flow field geometries to enhance water redistribution and pressure head losses reduction within PEM Fuel Cell

Kush Chadha, Serguei Martemianov, Anthony Thomas*
Institut Pprime, Université de Poitiers-CNRS-ENSMA, UPR 3346, 2 Rue Pierre Brousse, Bâtiment B25, TSA 41105, F-86073 Poitiers Cedex 9, France
(*) – corresponding author: anthony.thomas@univ-poitiers.fr

Abstract

Efficiency of fuel cell is dependent on reactant distribution, products evacuation, pressure losses and many of these factors is dependent on the design of flow field plate. With an effective design, reactant distribution, pressure drop and water and heat management can be further improved. In this work, two new designs, as multi-serpentine set-up with additional slots and hybrid geometry, on stainless steel bipolar plates, are presented. Electrical performance, and pressure head losses are analyzed by electrochemical methods such as polarization curve and use of electrochemical noise as a diagnostic tool to further understand the impact of water management on performance. Multi-serpentine design shows the best electrical performance whereas hybrid design reveals the lowest pressure head losses and higher stability that can be useful to downsize compressor and provide lower impact on fuel cell stack durability.

Keywords. Flow field geometry, Pressure head losses, Electrochemical noise**,** Statistical descriptors**,** PEM fuel cell

1. Introduction

Increasing energy concern related to environment pollution, rapid depletion of fossil reserves has led most of the research oriented to other alternative solutions. One of these is to explore polymer electrolyte membrane fuel cell (PEMFC) technology because of their ability to provide low-carbon electricity thanks to hydrogen vector (if hydrogen is product with low-carbon systems) and the only products as water and heat (that can be valorised). PEMFC advantages as low temperature operation (80°C), high power density (1 W/cm²) and low emission have led to opening new fields towards application of these systems. In order to further increase the efficiency (and durability) of these cells it is very important to understand the parameters on which the efficiency of fuel cell depends and what are the current drawbacks that PEMFC is face. An efficient working of fuel cell requires three main things, firstly homogeneous distribution of gases, secondly effective removal of water produced during operation, and thirdly low mass to power ratio. Most of these points can be enhanced with an efficient design of flow field, which can ensure homogeneity in terms of reactants, efficient removal of water and heat [1].

Traditional serpentine flow field geometry has shown good performance considering homogeneity of flow of gases in channels, but with number of bends produces larger pressure drop which ultimately effects the compressor efficiency [1]. Also due to number of bends, there is water accumulation across corners which can result in slug and plug in the way of reactant flow. Ijaodola *et al.* [2] presented work related to water flooding in PEMFC and how to promote proper water management. Ito *et al.* [3] highlighted results related to flooding in PEMFC gas diffusion layer by differential partial measurement. Quan *et al.* [4] explained water behaviour in serpentine micro-channel for proton exchange membrane fuel cell cathode and their results showed that water distribution in after bend might block the reactant supply to reaction sites. These results showed that it becomes important to explore other possible designs which can help an increase of efficiency and decrease in power consumption of fuel cell stack. Also, material of bipolar plate, plays an important role in analysing the overall efficiency of plates. Non-metallic (often carbon) and metallic bipolar plates are often used, and both classes have their own advantages [5, 6]. Carbon plate are the oldest but metallic plate are more and more used in fuel cell stack [7, 8].

Out of metallic, one of them mostly used is stainless steel bipolar plates as they show good electrical, mechanical and thermal properties but suffer from corrosion and a prolonged use of these plates can result in a very quick membrane poisoning which can be very detrimental to health of membrane. There have been a lot of research regarding coating for stainless steel bipolar plates considering material, thickness, chemical composition, effects [9-11]. Since the bipolar plates contribute 60-70 % of the total components of PEMFC stack therefore research is needed in this area to explore more feasibility with conductivity, heat management, vibration tolerant, flexural strength, impact strength, and overall weight of bipolar plates based on DOE targets.

Based on our search not much experiments and numerical analysis is carried on the channel design of flow field plates (FFPs) often named bipolar plates (BPPs). Key to efficiency is a good flow without dead zones in channels, effective distribution of reactants and lower pressure drop. Kloess *et al.* [12] worked on channel designs inspired from nature that result of a hybridization between serpentine and interdigitated designs. Interesting results were observed with an increase in power density at $T = 75°C$ and RH = 100% by 30%. Spiral geometry is also investigated by several groups. Ibrahimoglu *et al.* [13] investigated flow field design considering spiral geometry with less area in comparison of the standard area of serpentine plates (25 cm^2). Ansys Fluent PEMFC module is used to study this spiral design. The motivation behind this study is to identify the feasibility of circular shape PEMFC with a spiral flow-field design to increase the active area and to decrease auxiliary power consumption of the system, thereby understanding gas distribution, pressure distribution in membrane, anode and cathode flow channels. Cho *et al.* [14] used finite-element model of PEMFC with fractal branching. Idea is to optimised number of branching generations to homogenize reactant concentration. Behrou *et al.* [15] gave an interesting method using topology optimization to design flow field of PEMFC resulting in non-trivial optimised geometries. The objective function is to optimize both homogeneity of current density distribution and output power permitting reduced cost and increase in durability. Andrade *et al.* [16] gave a numerical solution using spiral geometry of flow channel. Using computational fluid dynamics code, finite volume scheme, various flow configurations were modelled ranging from 4 to 12 channels in multiple of 4 and simulated. They show that the 12 channel design give the maximum efficiency but higher pressure drop. Increase in inlet hydrogen velocity can increase the output performance of the cell. Compared current density at the entrance of fuel cell at same position shows the highest performance for radial in comparison to spiral and serpentine. Robles *et al.* [17] investigated the effect of spiral flow channel geometry in shape of 1, 2, 3, 4, 6 and 8 concentric spirals. Results were simulated by a three dimensional non-isothermal model, predicting water content and entropy generated in all zones inside the cell. Karthikeyen *et al.* [18] investigated experimentally zigzag positioned porous inserts on rib surface of cathode flow channel for performance enhancement. Those porous inserts which have 80 -90% porosity has improved the power density and current density by 11.5% and 7% respectively, compared to conventional serpentine channel. Nguyen [19] worked on gas distribution design to improve mass transport rates of reactants from flow channels to inner catalyst layers. Cooper *et al.* [20] examined critical cathode BPPs dimension such as channel/ land width, channel depth for both interdigitated and parallel designs and found that the most important parameter for interdigitated design which effects the raw power and limiting current density is stoichiometry, similarly for parallel channel design is channel/land width. Bipolar plates channel design was not only limited to rectangular dimensions as Khazaee *et al.* [21] worked on annular shaped geometries. The results by polarization are in good agreement with experiment. Interdigitated design is gaining attention in past years but yet to be fully understood. These designs promote forced convection, which helps to avoid flooding and gas diffusion limitations. Wang *et al.* [22] made performance studies with interdigitated flow fields and understood the effect of cell temperature, gas humidification, cell operating pressure and reactant gas flow rate on these designs. Based on their experimental conditions these designs work with good humidification,

increase in operation pressure. Carton *et al.* [23] worked on three-dimensional proton exchange membrane fuel cell model thereby providing a 3D CFD model for open pore cellular foam material. Results indicated that open pore cellular foam material plates distribute both hydrogen and oxygen more evenly from inlet to outlet, compared to double channel fuel cell. Wilberforce *et al.* [24] gave a detailed review considering distribution of various geometry designs and performance of PEMFC's. Geometric parameters for flow channel design plays a very important role for effective distribution and removal of reactants and on many more factors. Manso *et al.* [25] reviewed the influence of geometric parameters of flow fields and its performance on PEMFC. Following his work, flow field, flow direction, channel length and number of channels, use of baffles, cross sectional dimensions, rib width, channel depth, height to width ratio can have huge effect of performance of fuel cell.

Most of these studies use conventional electrochemical techniques, as polarization curve, interruption current and impedance measurements, to characterize performance and durability and design impacts on working fuel cells. Electrochemical techniques are easier to carry out and can give much detailed information. Of all the major problems, water flooding or drying of cell poses a major risk primarily because of durability issues [26]. To analyse in-situ water distribution, methods such as neutron imaging, x-ray, electron microscopy or optical photography are often used [27-29]. These techniques give a precious detailed view to understand more clearly the physic within the system but are expensive to carry out in a practical point of view. In this study, in addition to polarization curve analysis and pressure head losses measurements, a direct approach named Electrochemical Noise Analysis (ENA) is done by recording and analysing fluctuations of fuel cell parameters as voltage. Since this approach do not require use of costly instruments, easy to set anywhere and can be used upon any size of fuel cell and can give more faster results in varying conditions of fuel cell. ENA can be an important tool to understand the flooding and drying behaviour of fuel cell [30, 31].

Maiza *et al.* [30] worked on similar procedure, case of flooding condition to check how the signals can vary with the accumulation or poor removal of water in the cell. Mortazavi *et al.* [32] worked on similar approach to understand the liquid gas two-phase flow pressure drops in ex-situ fuel cell setup. The aim of the work was to understand pressure drop signatures with different flow rate within a flow channel. Mishima *et al.* [33] developed a study to understand flow regime, void fraction, and velocity rise of slug bubbles in capillary tube with inner diameters ranging from 1 to 4 mm. Mansfeld *et al.* [34] evaluated coating degradation with electrochemical impedance spectroscopy and electrochemical noise analysis on cold rolled steel. Martemianov *et al.* [35] worked on similar methodology of noise analysis and application for commercial Li-ion batteries. Baert *et al.* [36] worked on noise voltage of batteries. Gabrielli *et al.* [37] developed model of the stochastic behaviour of electrochemical interface governed by chemical or electrochemical reactions. Rubio *et al.* [38] studied PEMFC failure mode of earlier diagnosis with wavelet analysis of electrochemical noise. Analysis of electrochemical noise, in some cases for example in cases of flooding shows a drift in signal which can be due to low frequency component of signal, Bertocci *et al.* [39] analysed and discussed various drift removal procedures. Electrochemical noise analysis as a tool is used in many studies to explore the irregularities and possibilities of defects [40-42].

The aim of the present work is to study new geometries impact on performance and pressure drops and analyse the results obtain in comparison of conventional techniques and instrument. For the first part of article the designs effect will be analysed with polarization curve and electrochemical noise measurements. ENA will be perform with the evolution of temporal descriptor as standard deviation (STD) This will be help, qualitatively and quantitatively, to understand the designs impacts with respect to an easier water removal. In the second part pressure head losses will be evaluated and compared between each design.

The paper is organized in the following way. The "Experiment" section presents the three designs used and experimental details of the provided experiments. In the "Electrochemical noise methodology" section, the details the evaluation of noise and the detrending procedure of noise are presented. The robustness of obtained statistical descriptors as time windows is considered. Results of polarization curve of the three design, electrochemical noise analysis and head pressure losses are given in the "Results" section. Conclusions of the present work and some perspectives are specified in the "Conclusion" section

2. Experiment

2.1 Bipolar plate designs

In this research two new designs of bipolar plate are compared with traditional serpentine (Fig. 1). The plates have been named in order to highlight the use. Fig. 1a represents the traditional serpentine geometry, Fig. 1b multiple serpentine (multi-serpentine) geometry with additional slots and Fig. 1c hybrid (serpentine + parallel) design. The choice of this design are explained below.

Traditional serpentine design suffers from various flooding and drying of membrane issues. Le *et al.* [43] presented results regarding the liquid water behaviours in proton exchange membrane fuel cell cathode with serpentine channels. Lee *et al.* [44, 45] gave radiographic investigations of liquid water transport behaviour in PEMFC. Aslam *et al.* [46] simulated similarly for direct visualization of liquid water in PEMFC's. Extensive research has been published so far regarding the use of this plates with both performance, modification and drawbacks [47-49].

Multiple serpentine geometry with additional slots (Fig. 1b) are developed to enable homogeneous water distribution. Multi-serpentine designs have already analyzed in literature [50] by analyzing the optimum channel length for flow but not with slots addition. There is no accurate way to understand the water distribution in the bipolar plate accurately and precisely. A typical

multi-serpentine channel has 4-8 channels in parallel to avoid long channel lengths and hence reduced pressure head losses, however if any one channel in multi-serpentine channel is blocked, there will be different possible cases :

- Reactants will be forced to move from the gas diffusion layer, inducing more pressure head and non-uniformity of pressure on the gas diffusion layer.
- Due to blockage by water, there is a possibility that the entire length which was supposed to carry the reactants will be without any reactants and hence again a non-uniform distribution on the gas diffusion layer.

In a fuel cell working at a relative humidity of 100% or working at high currents with an high water production, this water needs to be flushed out to avoid flooding. For example, in multi-serpentine plates with size of 10 cm × 10 cm if a channel is blocked with slug or plug it will block the entire channel to further carry the reactants and decrease the reactions surface of electrodes that impact performance. In the present work slots are added to the multi-serpentine design to avoid slug formation. Indeed, if a channel is blocked, the slug thanks to the added slots, can redistribute into smaller droplets and can make a way forward for further reactants to distribute homogenously.

Hybrid design (Fig. 1c), to take into the effect of the pressure losses, promote homogeneity, and ease in water removal. The idea behind using this design is to reduce the serpentine long lengths and equally replacing by exterior parallel channels to promote faster water removal and gas distribution and decrease pressure head losses.

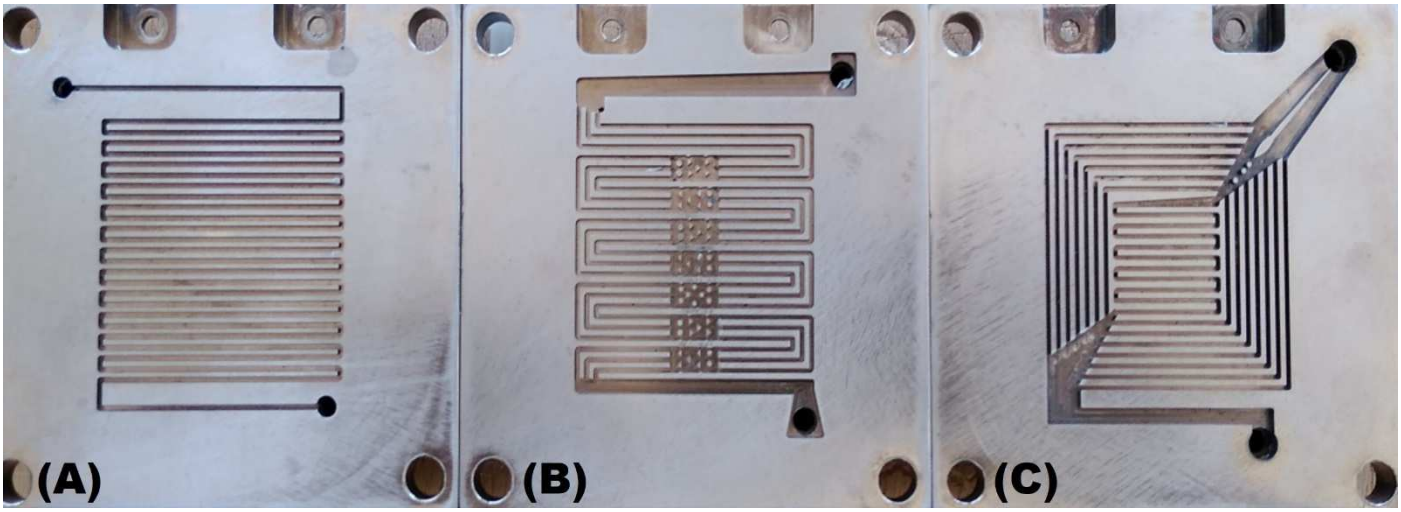

Fig. 1 (a) traditional serpentine design (b) multi-serpentine design (with slots) and (c) hybrid design. Active area = 25 $cm^{2.}$ Depth of channel is 2 mm.

2.2 Experimental setup

Fig. 2 presents the experimental setup used for our experiments. For the fuel cell assembly, metallic stainless steel 316L flow field pates are used. A carbon-based coating material developed by Precors® is used on the plates. Thickness used for the coating is 100 nm. Tests are carried out using Nafion® NRE-211 membrane, GDL Sigracet® 39 BC, for a fuel cell temperature of 60°C and relative humidity at the inlet set to 50%. Each bipolar plate has an area of 100 cm^2 (10 cm x 10 cm) and effective reaction area of 25 cm^2 (5 cm × 5 cm). Lands and channels are divided in ratio of 50%. Depth of channel is 2 mm. Gas used at anode is hydrogen and at the cathode side is pure oxygen, connected by flow meters to regulate the amount of flow based upon the current applied. Stoichiometry for hydrogen is set to 1.4 and for pure oxygen is set to 1.2. Two separate humidifiers are used to maintain the right amount of humidity for effective working of fuel cell operations. A temperature controller was used to maintain the required amount of relative humidity in the fuel cell. The connection between humidifiers and fuel cell are preheated to avoid the condensation of water present within humidified gases which can result flooding issues at the inlet of the cell. Temperature of preheating is set to 65°C. Thermo-regulation is used to maintain the fuel cell at 60°C on both the sides of stainless steel BPPs thanks water circulation. Special C-clamps are used to hold the two plates together. It is made sure that equal compression is given to all the three sets of bipolar plates. Isoflon® gasket, thickness 0.25 mm is used to avoid gas leakage and insulation. Pressure sensors JUMO MIDAS® are connected both at hydrogen and oxygen inlet of PEMFC to measure the inlet pressure. The outlets are open to the atmosphere. Pressure sensors have range of 250 kPa and accuracy of 0.25 kPa. To impose current in galvanostatic mode an electronic load, Kikusui® PLZ664WA 0-150 V 0-132 A is used. Electrochemical data, except polarization curve, is collected at two operating current value of 4A and 19A (corresponding to 0.16 A/cm^2 and 0.76 A/cm^2 respectively) during 2 hours for each point. In order to record the signals of pressure and fuel cell voltage fluctuation for ENA, a National Instruments data acquisition card NI DAQ 9234 is used which has a 24-bit resolution for good accuracy and sensitivity of measurement with anti-aliasing filter. All data of pressure and voltage are recorded with a 2048 Hz frequency and using LabView®. Matlab® and Python® are then used for further signal treatment.

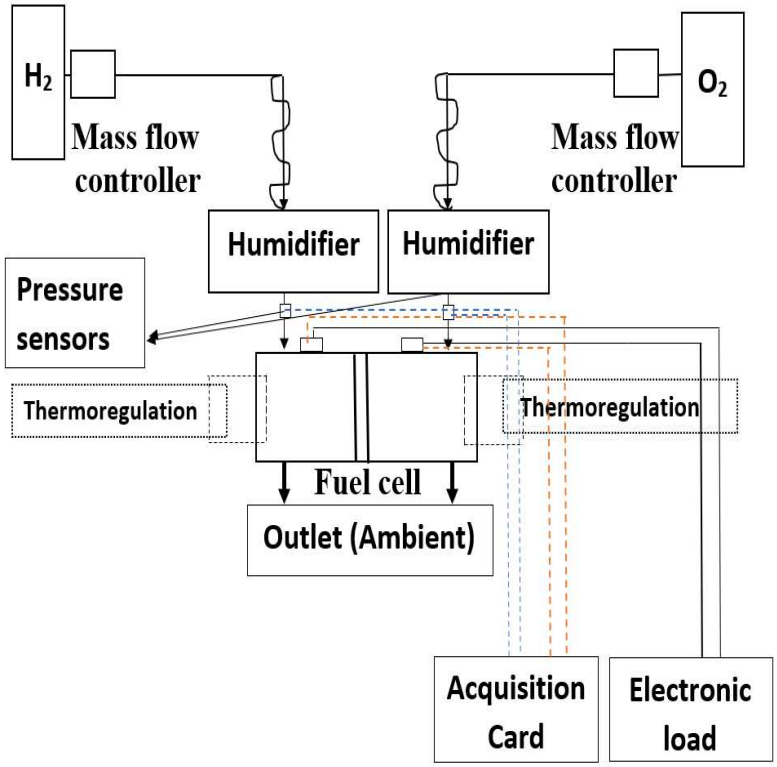

Fig. 2 Schema of experimental setup

3. Electrochemical noise methodology

3.1 Intrinsic noise

In order to characterize electrochemical noise of fuel cell, it is very important to estimate the intrinsic noise of experimental setup, on the basis of magnitude of energy (intensity) of signals captured (Fig. 3a). Hence, in order to differentiate the noise of bench and the electrochemical noise of fuel cell working, measurements have been performed with fuel cell feed with gases with active electronic load set at 4A named ON and without gases named OFF. The data recorded shows a peak to peak voltage of 40 mV for the fuel cell ON (Fig. 3b) and 4 mV for the fuel cell OFF (Fig. 3c) condition which is roughly 10 times higher. This confirm that the fuel cell noise can be measured by our acquisition system with enough intensity of the fuel cell signal.

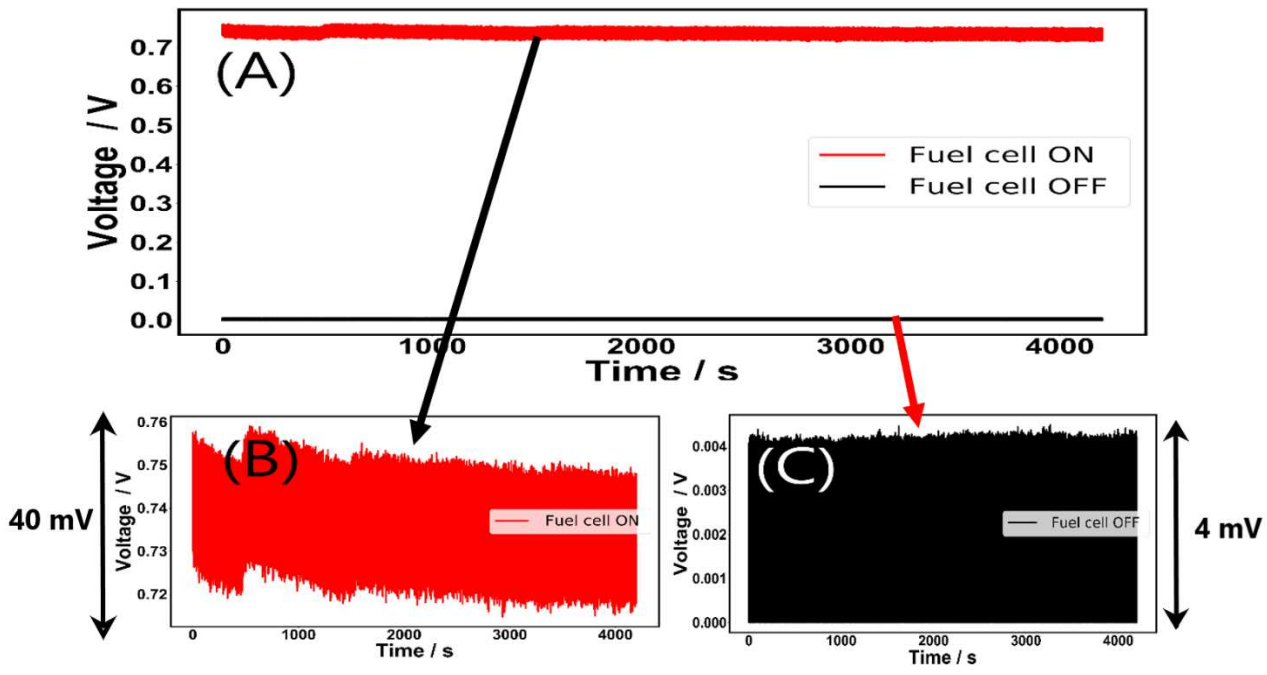

Fig.3 (a) Evolution of voltage fluctuation of fuel cell running (ON) and bench noise without any reactants (OFF). Enlarged version and their magnitude of (b) fuel cell voltage at 4 A (0.16 A/cm²) (c) bench noise.

3.2 Signal detrending procedure

Time varying trends can contain useful information on the evaluation of signal which can show both slow dynamic (low-frequency) variations and fast dynamic (high frequency) variations. In order to understand the electrochemical signal, it is important to detrend signal function therefore isolating noise. Detrending as a tool have been used to remove trends in electrochemical noise [51-53]. In order to study and apply stationary methods, in the present work, signal is detrend with a linear polynomial in python SciPy module. For that the 2 hours signal (7200 seconds) is broken down to 200 seconds window (36 parts) and then an individual linear fit is performed for each part of data between two break points. Linear mode calculates the linear least-squares fit to data and subtracts from data in the given time window. Fig 4 shows the evolution of voltage signal at 19 A (0.76 A/cm²) and detrend signal for serpentine design. It is chosen to highlight detrending procedure with the less table signal as voltage signal measurement at 19 A for serpentine design. The voltage decreases from 0.25 to 0.15 V for the 4800 first seconds and after some peaks until 0.20 V appears for a period of about 1000 s. As evident from Fig. 4, after applying the linear detrend procedure, it removes certain trend however some form of fluctuations especially for the peaks impact a little bit the detrend. Sure, the number of parts and the order of polynomial impact the detrend procedure [52]. To see the impact of detrend procedure some comparison has been made in the next section.

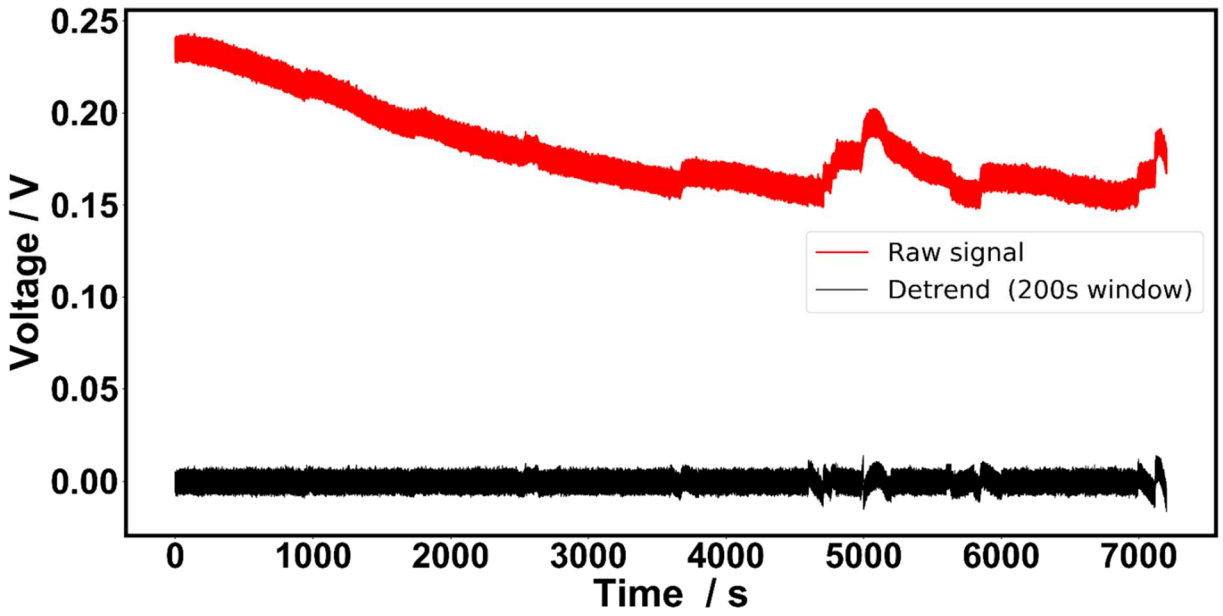

Fig. 4 Evolution of voltage signal at 19 A (0.76 A/cm²) and detrend signal for serpentine design

3.3 Time window comparison

Working with electrochemical noise is mainly working with stochastic signals, which have no preferred outcome, or which cannot be determined. It becomes important to analyse the signal while breaking into stationery points and choosing an appropriate time window. Indeed, electrochemical noise has a problem issue related to the non-stationary character of the signal [54, 55]. One of the possibilities to solve this problem is using short-time analysis [56, 57].

The same procedure through short-time analysis as our previous work [57] is followed in this work, to guarantee the stability and relevance of the signal detrending. Four size of time windows have been tested (18, 72, 200 and 400s) that divided respectively in 400, 100, 36 and 18 parts. As an adapted filter, the choice of the size of the windows can allow to filter the low frequency or high frequency part of the signal, depending of your time constant looking. The more your time windows is tiny the more you cut your low frequency (as an high-pass filter). If your system has a long time constant it is preferable to use large time windows and reversely if your time constant is short. The choice to use a direct measurement (DC) of the signal and apply specific detrending procedure and statistical descriptor calculation as standard deviation (STD) in this present work is to be sure of the impact our acquisition system. When a filter is used to measured signal (AC) associated often to amplifier, the impact of the filter in most of the case is never considered.

Fig. 5 highlights the effect of the size of time window on the detrending of the signal. The same signal of voltage fluctuations at 19 A for serpentine design recorded during 7200 s as Fig. 4 is used for the comparison. It can be seen (Fig.5a) that when a 400 s time window is used, some large fluctuations is always apparent near 5000 and 7000 seconds, corresponding to the large peaks on the raw signal (Fig. 4). When the size of the time window is reduced to 200 s the peaks influence decreases, but large fluctuation remains on the detrend signal. From a time window size of 36 s and after 18 s, no large fluctuations are noticeable on the detrend signal, due to an higher filtering of the signal when small windows are used. Fig. 5b shows the comparison of the four detrend signals with time windows of 400, 200, 72 and 18s. It is clear that all the signals are centred in 0 V and 200 and 400 s time window detrend signal show large fluctuations between -0.015 and 0.015 V due to the effect of the low frequency peaks within the raw signal (Fig. 4). STD evaluation (Fig. 5c) highlights this behaviour and reveals large peaks between 4 and 5 mV near 5000, 5700 and 7200 s. For the time windows of 72 s, STD peaks are lower except at 7200s. For the time windows of 18 s, this time

windows size is too tiny and a flat evolution of STD is obtained. Because in this paper ENA will be evaluated thanks to the evolution of STD with time for the three different design and the aim is to track the effect of the design on water management, it is chosen to use a time window of 200 s to detrend the signal, to not filter too much the low frequency and cancel the presence of low frequency peaks on the signals. Indeed, presence of slug or plug within the flow field channel shows a large time constant (several seconds to several minutes, depending on length and geometry of flow field plate) [58-60].

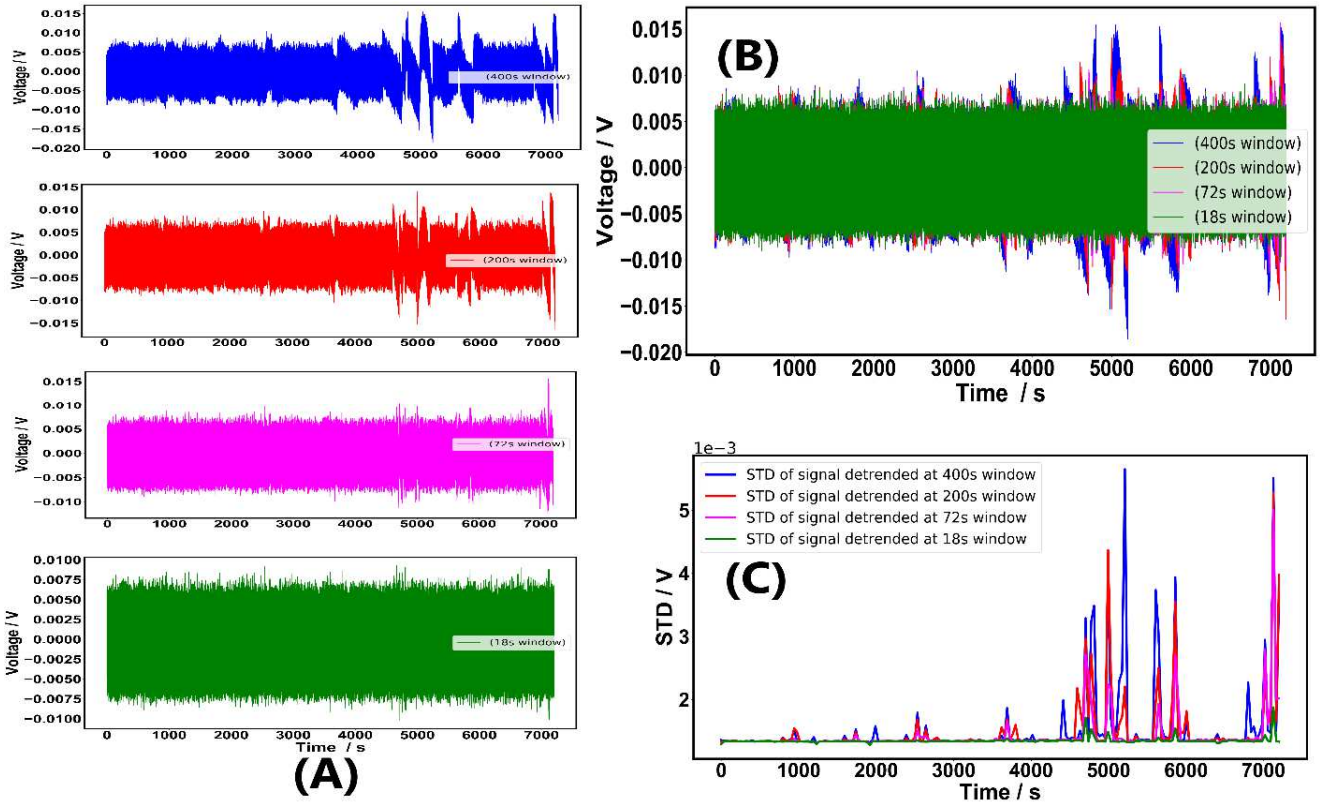

Fig. 5 Effect of time windows on detrend calculation

It can be precise that for all STD calculations presented in Fig. 5c, a window of 36s seconds was chosen. Indeed, there is two steps to calculate STD in our procedure. First, the signal is detrend choosing a size of time window and applying a linear polynomial to subtract the mean value of the raw signal. And secondly, the STD is calculated on the detrend signal choosing an accurate window to calculate the STD.

Fig. 6 highlights the influence of the window on STD estimation for the 200 s window detrended signal. Four value of windows is chosen to calculate STD, 18, 36, 72 and 200 s. Sure it can be noted that when a window of 200 s is chosen for a 200 s window detrended signal, only few values (36 exactly) of STD are calculated. If the time of the windows is decreased to 72, 36, 18 richer information and more peaks with higher values appear, especially where low-frequency peaks are present within the raw signal (near 5000, 6000 and 7200 s – Fig. 5a). The choice of the size of the time windows to calculate the STD must be done on a stability criterion (can be relative). It means when the decrease the size of the windows continue to reveal new peaks, size of window can be decreased. When the decreasing of windows size does not affect a lot the number of peak (only affect the absolute value of the peak) STD calculation start to be stable. Regarding Fig. 6, a windows size of 36s is chosen to calculate the STD evolution with time for all results presented in “Results” section. The time windows of 36 seconds provided, in our point of view, the most relevant information on standard deviation (STD) of the measured signals that linked to the intensity of the signals.

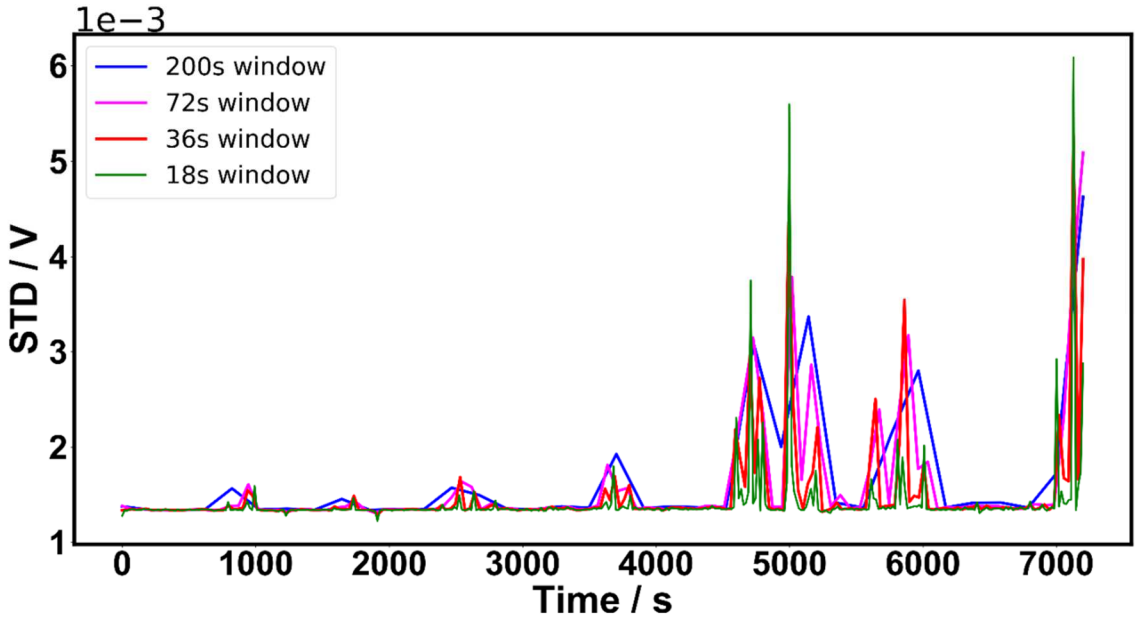

Fig. 6 Influence of windows on STD estimation

4. Results and discussion

4.1 Polarization test

Polarization curves are generally used to describe the phenomenon of electrochemical reactions and to characterize the fuel cell. This can be a very important tool to understand the kinetics, resistance and mass transfer of a fuel cell. Based upon this, important observations can be withdrawn explaining what the source of global performance losses in can be working of fuel cell. The polarization curve of the three designs are presented in Fig. 7. The activation losses, which occur at low current densities (< 0.2 A / cm^2), are similar for all three designs except multi-serpentine geometry shows less losses to begin the reaction. Major difference regarding fuel cell performance can be seen in ohmic part (linear part). Fig. 7 highlights that multi-serpentine geometry give the best electrical performance. The multi-serpentine design demonstrates a voltage of 0.65 V compared to 0.6 V to the hybrid and 0.58 V to the serpentine cell at 0.4 A/cm^2, and of 0.5 V compared to 0.3 V and 0.25 V at 0.9 A/cm^2, respectively. The ohmic loss is mostly significant for the case of serpentine geometry which is followed by hybrid in comparison of multi-serpentine mostly due to a higher membrane resistance.

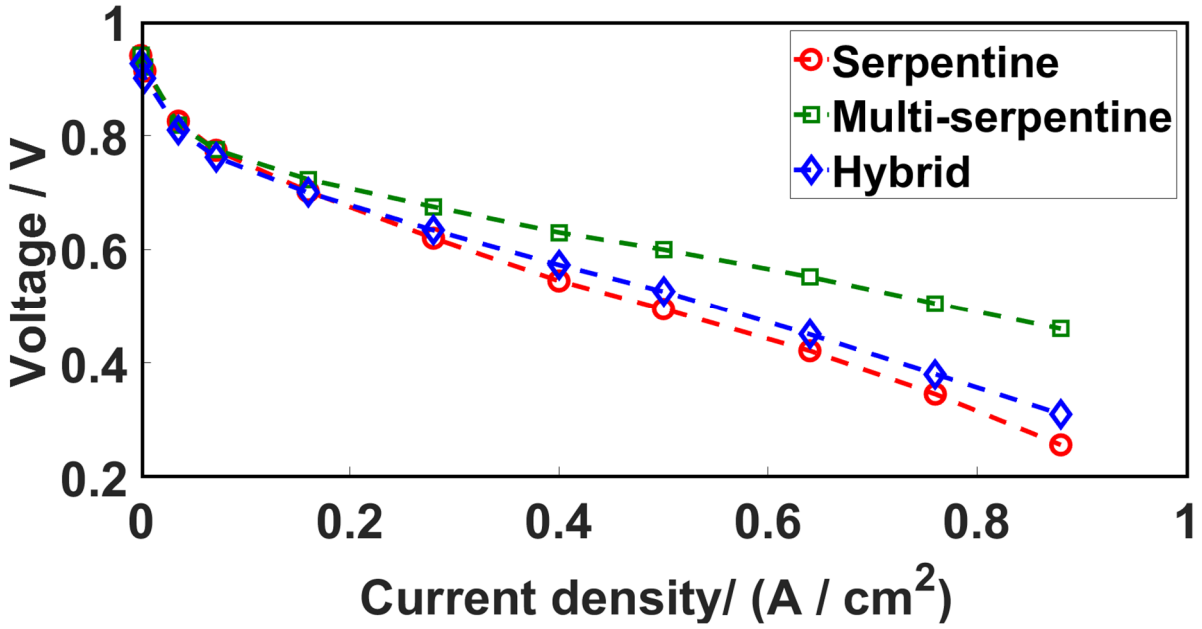

Fig. 7 Polarization curve comparison for the three designs

4.2 Electrochemical noise analysis applied to three geometries through STD evolution of voltage signals

Standard deviation (STD) can be a good descriptive tool, describing the intensity of noise signal, which can explain how data for a signal are spread out from average or mean. Similiarly a low STD value explains signals are mostly close to mean and a high value explains far away from mean. In order to understand the impact of different flow field design, noise as a tool can give vital information for diagnostic perspective [61], especially considering the effect of water management [30, 57], flow of gases [62] and current [63]. Electrochemical noise analysis offers promising possibilities allowing in-situ diagnosis of electrochemical energy sources, without system perturbations [64].

As mentioned above in all the experiments the electrochemical noise is recorded directly to understand the signature and its impact on temporal analysis. For temporal analysis STD calculation on a time windows of 36 seconds, on a signal detrend with 200s linear polynomial subtraction window, are used to evaluate the intensity of voltage signals and follow the STD variations over the entire measured signals that have a duration of 7200s for each experiment. Two operating point are used at a current of 4 A (0.16 A/cm²) and at 19 A (0.76 A/cm²) for three geometry: serpentine, multi-serpentine and hybrid.

In a qualitative point of view, Fig. 8 presents the voltage signals for the three geometry. Two regime are distint, at 4 A (0.16 A/cm² - Fig. 8a,b,c) where the kinetic effects are predominant and at 19 A (0.76 A/cm² - Fig. 8d,e,f). At 4 A, low frequency voltage fluctuations are lower in comparison at 19 A. That can be due to a higher impact of the water management (due to higher amount of water produced) at 19 A. In a geometry comparison point of view, serpentine highlights the lowest stability, especially at 19 A (Fig. 8d), followed by multi-serpentine (Fig. 8e) and hybrid design give a great stability with no low-frequency fluctuations at 19 A (Fig. 8f). The stable evolution of the voltage within hybrid design can be due to a more uniform repartition of pressure and higher amount of pathway for gases due to the central parallel design of this hybrid geometry.

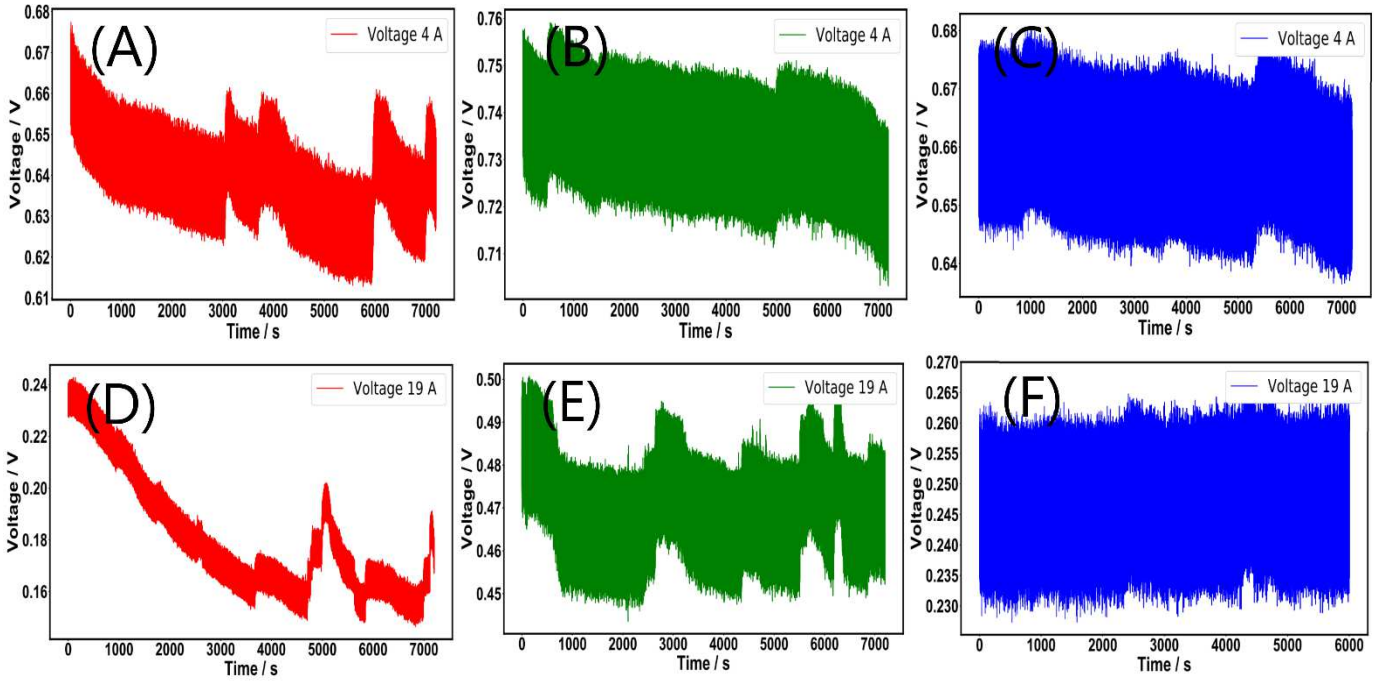

Fig. 8 Raw voltage signals evolution at 4A (0.16 A/cm²) for (a) serpentine (b) multi-serpentine and (c) hybrid design and at 19A (0.76 A/cm²) for (d) serpentine (e) multi-serpentine and (f) hybrid design

In a quantitative point of view, Fig. 9 shows the STD fluctuations of the voltage signals for the three geometry presented Fig. 8. In overall, STD values are near the value of 3mV, excepted at a value of 1.3 mV for the serpentine geometry at 19 A. In the fluctuation of STD values point of view, as raw voltage measurement (Fig. 8), the traditional serpentine geometry present the noisiest signature. More peaks and higher standard deviation values at 4A (Fig. 9a) and 19A (Fig. 9d) are highlighted, which is less for multi-serpentine, some peaks with less intensity are present at 19A (Fig. 9e) and no variation or presence of peaks for hybrid design. The apparence of STD peaks and high values is due to a non-optimised water management has shown in our previous work [57].

These behavior characterize by the STD evolution of voltage signals give us the signature of the three geometries. For serpentine design, an interpretation of this high fluctuating behavior can be due that, considering flow only in one channel, water is forced to move in one direction and if slug or plug appears that involve more irregularities in voltage signalsand so STD peaks appears (Fig. 9 a,d). For multi-serpentine 4A results shows no fluctuations (Fig. 9b) and 19A (Fig. 9e) shows fluctuations but the magnitude is less then traditional serpentine. The reason of this behavior can be attributed to the re-distribution of water in the slots which results in more stable voltage. The stable behavior on voltage signals for hybrid design can be due to an easier removal of water, where it is not forced to follow a fixed trajectory and can correctly distributed at the inlet due to the presence of

parallel channel. Also, hydrid combine advantages of parrallel and serpentine geometry which furthers distribute the water distribution.

Wua *et al.* [65] has published results using neutron imaging to study water removal in single, double and quad channel serpentine based geometry. They report an ineffective liquid water removal for quad design and in our study based on electrochemical noise analysis, it is seen a stable voltage at lower current and some disturbance at higher currents. This is in agreement with their results, however they founded better performance for serpentine compared to quad channel. In the present study introduction of slots in multi-serpentine channel design can be a reason for better performance and stability compared to serpentine as slots allow more paths for removal of accumulated water. Again, considering neutron imaging results, Spernjak *et al.* [66] comparing serpentine, parallel and interdigitated, shows that serpentine give better performance considering the removal of accumulated water with time. Since parallel geometry suffers poor water removal hence in our study, hybrid design, combining parallel and serpentine, shows better performance in voltage and STD fluctuations point of view compared to serpentine and multi-serpentine modified with slots.

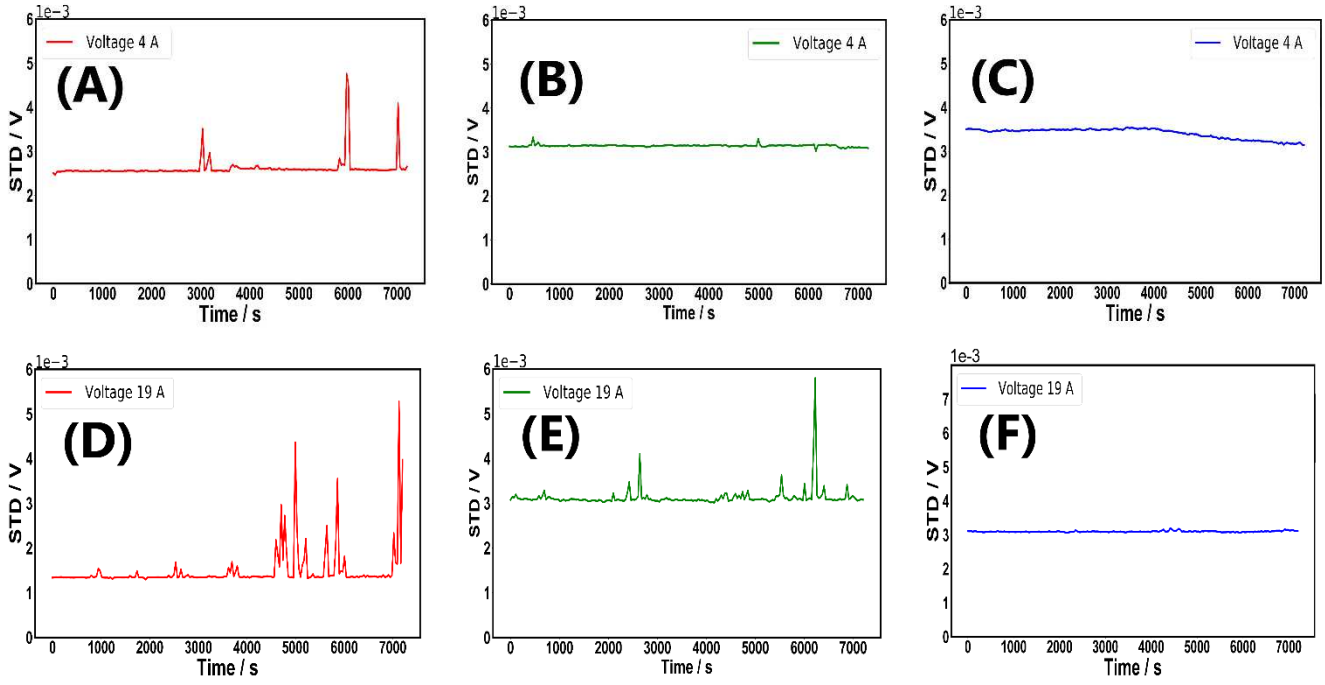

Fig. 9 Voltage standard deviation evolution at 4A (0.16 A/cm²) for (a) serpentine (b) multi-serpentine and (c) hybrid design and at 19A (0.76 A/cm²) for (d) serpentine (e) multi-serpentine and (f) hybrid design

4.3 Pressure drops for different geometries

Fig. 10 shows the mean pressure drop values over anode side (Fig. 10a) and cathode side (Fig. 10b). For all an error limit is put to take in account the precision and sensitivity of the pressure sensor. For both side, serpentine shows the highest head losses pressure with a variation between 4.7 to 5.7 mbar at anode side and variation between 2 to 2.4 mbar at cathode side. At higher currents (19A), a decrease in pressure head loss is observed at the anode side (Fig. 10a). Multi-serpentine geometry gives stable and lower pressure head losses near 4.2 mbar at anode side and 1.2 mbar at cathode side. Hybrid geometry highlights the lowest pressure drop difference with stable value near 3.3 mbar at anode side. For cathode side, a value of 0.7 mbar at 4A and 0 mbar are measured. The value 0 at 19A is due to the error limit of (± 0.7) mbar and offset precision of the pressure sensor. Hence it is assumed that with present sensor accuracy limit it is not suitable to calculate the pressure drop limit for hybrid design at 19 A. In overall, results show that serpentine geometry has highest pressure head losses and minimum for hybrid design. Pressure head losses are lower at cathode side compared to anode side because pure oxygen (flow rate divided by two) are used. Pressure measurements here are mainly limited to single cell and a clearer picture can be provided by testing in stack considering the pressure head losses or cells having higher area.

It can be noted that serpentine although is the most traditional used geometry suffers higher-pressure head losses and hence it directly effects the compressor power in the fuel cell stack. Pei et al [26] reviewed water fault diagnosis of PEMFC associated with pressure drop and gave useful descriptor regarding flooding or dehydration of fuel cell based upon the pressure drop information. Grimm et al [67] modelled gas flow in PEMFC channels and observed the flow pattern transitions and pressure drop through GDL.

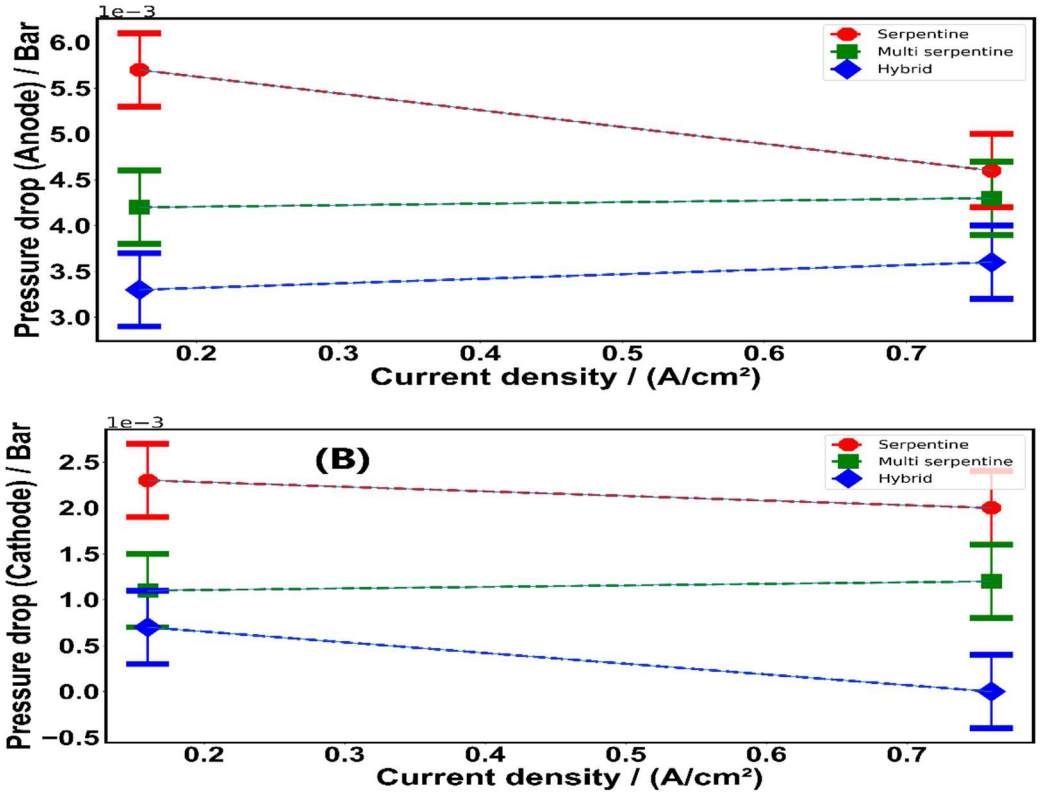

Fig. 10 Pressure drop variations for the three designs (a) for anode side and (b) for cathode side

5. Conclusion

Traditional serpentine geometry of flow field plate is compared to two novel geometry (multi-serpentine with slots and hybrid geometry) in this paper. Classical analysis as polarization curve comparison and pressure drops measurements are presented. Results show that best electrical performance is obtained for multi-serpentine flow field plate design set up with slots. Hydrid design, that takes advantages of serpentine geometry and parallel geometry, highlights the lower pressure drops with reasonable electrical performance that, in overall, leads to higher performance for fuel cell stack integration with the use of smaller air compressor.

Moreover, electrochemical noise analysis was applied to voltage measurements for two operating point. Based on the signals obtained, qualitative and quantitative analysis was performed in temporal domain thanks to standard deviation variations with short-time analysis. Considering the case of voltage signals, qualitative analysis of three geometries shows a maximum disturbance in serpentine geometry, followed by multi-serpentine geometry set-up with slots and mostly stable fluctuations for hybrid geometry. Hybrid design highlights the higher stability with no presence of large fluctuations of peaks, that is a signature of good water management. Serpentine geometry reveals the lowest stability and highest presence of peaks due to worse removal of water. Multi-serpentine design helped with the addition of slots shows a reasonable stability of voltage fluctuations and good performance. The new flow field geometries proposed in this work to enhance water redistribution and reduction in pressure head losses in this paper can be a first step for further flow field plate designs development in fuel cell stacks area. To go further concomitant measurement and cross-measurements of pressure, impedance and temperature evolution and correlation between signals for several operating point and relative humidities will be done in a future work.

References

[1] Li X, Sabir I (2005) Review of bipolar plates in PEM fuel cells: Flow-field designs. Int J Hydrogen Energy 30:359-371. https://doi.org/10.1016/j.ijhydene.2004.09.019

[2] Ijaodola OS, El-Hassan Z, Ogungbemi E, Khatib FN, Wilberforce T, Thompson J, Olabi AG (2019) Energy efficiency improvements by investigating the water flooding management on proton exchange membrane fuel cell (PEMFC). Energy 179:246-267. https://doi.org/10.1016/j.energy.2019.04.074

[3] Ito K, Ashikaga K, Miyazaki T, Ohshima H, Kakimoto Y, Masuda H, Sasaki K (2008) Estimation of flooding in PEMFC gas diffusion layer by differential pressure measurement. J Power Sources 175:732-738. https://doi.org/10.1016/j.jpowsour.2007.10.019

[4] Quan P, Zhou B, Sobiesiak A, Liu Z (2005) Water behavior in serpentine micro-channel for proton exchange membrane fuel cell cathode J Power Sources 152:131-145. https://doi.org/10.1016/j.jpowsour.2005.02.075

[5] Wang H, Turner JA (2016) Chapter 13 Materials for PEMFC Bipolar Plates Fuel Cells : Data, Facts and Figures. Wiley Online Library https://doi.org/10.1002/9783527693924.ch13

[6] Song Y, Zhang C, Ling CY, Han M, Yong RY, Sun D, Chen J (2019) Review on current research of materials, fabrication and application for bipolar plate in proton exchange membrane fuel cell. Int J Hydrogen Energy https://doi.org/10.1016/j.ijhydene.2019.07.231

[7] Richards J, Cremers C, Fischer P, Schmidt K (2012) Corrosion studies on electro polished stainless steels for the use as metallic bipolar plates in PEMFC applications. Energy Procedia 20:324-333. https://doi.org/10.1016/j.egypro.2012.03.032

[8] Yi P, Peng L, Zhou T, Wu H, Lai X (2013) Development and characterization of multilayered Cr–C/aC: Cr film on 316L stainless steel as bipolar plates for proton exchange membrane fuel cells. J Power Sources 230:25-31. https://doi.org/10.1016/j.jpowsour.2012.11.063

[9] Jannat S, Rashtchi H, Atapour M, Golozar MA, Elmkhah H, Zhiani M (2019) Preparation and performance of nanometric Ti/TiN multi-layer physical vapor deposited coating on 316L stainless steel as bipolar plate for proton exchange membrane fuel cells. J Power Sources 435:226818. https://doi.org/10.1016/j.jpowsour.2019.226818

[10] Gago AS, Sanchez DG, Ansar AS, Gazdzicki P, Wagner N, Arnold J, Friedrich KA (2015) Improved Water Management with Thermally Sprayed Coatings on Stainless Steel Bipolar Plates of PEMFC. ECS Transactions 69:223-239. https://doi.org/10.1149/06917.0223ecst

[11] Asri NF, Husaini T, Sulong AB, Majlan EH, Daud WRW (2017) Coating of stainless steel and titanium bipolar plates for anticorrosion in PEMFC: A review. Int J Hydrogen Energy 42:9135-9148. https://doi.org/10.1016/j.ijhydene.2016.06.241

[12] Kloess JP, Wang X, Liu J, Shi Z, Guessous L (2009) Investigation of bio-inspired flow channel designs for bipolar plates in proton exchange membrane fuel cells. J Power Sources 188:132-140. https://doi.org/10.1016/j.jpowsour.2008.11.123

[13] Ibrahimoglu B, Yilmazoglu MZ, Celenk S (2017) Investigation of spiral flow-field design on the performance of a PEM fuel cell. Fuel Cells 17:786-793. https://doi.org/10.1002/fuce.201700076

[14] Cho JIS, Marquis J, Trogadas P, Neville TP, Brett DJL, Coppens MO (2019) Optimizing the architecture of lung-inspired fuel cells. Chem Engineering Science 115375. https://doi.org/10.1016/j.ces.2019.115375

[15] Behrou R, Pizzolato A, Forner-Cuenca A (2019) Topology optimization as a powerful tool to design advanced PEMFCs flow fields Int J Hydrogen Energy 135:72-92. https://doi.org/10.1016/j.ijheatmasstransfer.2019.01.050

[16] Cano-Andrade S, Hernandez-Guerrero A, Von Spakovsky MR, Damian-Ascencio CE, Rubio-Arana JC (2010) Current density and polarization curves for radial flow field patterns applied to PEMFCs (Proton Exchange Membrane Fuel Cells). Energy 35:920-927. https://doi.org/10.1016/j.energy.2009.07.045

[17] Juarez-Robles D, Hernandez-Guerrero A, Ramos-Alvarado B, Elizalde-Blancas F, Damian-Ascencio CE (2011) Multiple concentric spirals for the flow field of a proton exchange membrane fuel cell. J Power Sources 196:8019-8030. https://doi.org/10.1016/j.jpowsour.2011.05.029

[18] Karthikeyan P, Vasanth RJ, Muthukumar M (2015) Experimental investigation on uniform and zigzag positioned porous inserts on the rib surface of cathode flow channel for performance enhancement in PEMFC. Int J Hydrogen Energy 40:4641-4648. https://doi.org/10.1016/j.ijhydene.2015.01.175

[19] Nguyen T V (1996) A gas distributor design for proton-exchange-membrane fuel cells. J Electrochem Soc 143:L103. https://doi.org/10.1149/1.1836666

[20] Cooper NJ, Smith T, Santamaria AD, Park JW (2016) Experimental optimization of parallel and interdigitated PEMFC flow-field channel geometry. Int J Hydrogen Energy 41:1213-1223. https://doi.org/10.1016/j.ijhydene.2015.11.153

[21] Khazaee I, Ghazikhani M (2011) Performance improvement of proton exchange membrane fuel cell by using annular shaped geometry. J Power Sources 196:2661-2668. https://doi.org/10.1016/j.jpowsour.2010.11.052

[22] Wang L, Liu H (2004) Performance studies of PEM fuel cells with interdigitated flow fields. J Power Sources 134:185-196. https://doi.org/10.1016/j.jpowsour.2004.03.055

[23] Carton JG, Olabi AG (2017) Three-dimensional proton exchange membrane fuel cell model: comparison of double channel and open pore cellular foam flow plates. Energy 136:185-195. https://doi.org/10.1016/j.energy.2016.02.010

[24] Wilberforce T, El Hassan Z, Ogungbemi E, Ijaodola O, Khatib FN, Durrant A, Olabi AG (2019) A comprehensive study of the effect of bipolar plate (BP) geometry design on the performance of proton exchange membrane (PEM) fuel cells. Renewable and Sustainable Energy Reviews 111:236-260. https://doi.org/10.1016/j.rser.2019.04.081

[25] Manso AP, Marzo FF, Barranco J, Garikano X, Mujika MG (2012) Influence of geometric parameters of the flow fields on the performance of a PEM fuel cell. A review. Int J Hydrogen Energy, 37:15256-15287. https://doi.org/10.1016/j.ijhydene.2012.07.076

[26] Pei P, Li Y, Xu H, Wu Z (2016) A review on water fault diagnosis of PEMFC associated with the pressure drop. Applied Energy 173:366-385. https://doi.org/10.1016/j.apenergy.2016.04.064

[27] Cochet M, Forner-Cuenca A, Manzi V, Siegwart M, Scheuble D, P. Boillat (2018) Novel Concept for Evaporative Cooling of Fuel Cells: an Experimental Study Based on Neutron Imaging. Fuel Cells published online. https://doi.org/10.1002/fuce.201700232

[28] Meyer Q, Ashton S, Boillat P, Cochet M, Engebretsen E, Finegan DP, Lu X, Bailey JJ, Mansor N, Abdulaziz R, Taiwo OO, Jervis R, Torija S, Benson P, Foster S, Adcock P, Shearing PR, Brett DJL (2016) Effect of gas diffusion layer properties on water distribution across air-cooled, open-cathode polymer electrolyte fuel cells: A combined exsitu X-ray tomography and in-operando neutron imaging study. Electrochim Acta 211:478-487. https://doi.org/10.1016/j.electacta.2016.06.068

[29] Ge N, Banerjee R, Muirhead D, Lee J, Liu H, Shrestha P, Wong AKC, Jankovic J, Tam M, Susac D, Stumper J, Bazylak A (2019) Membrane dehydration with increasing current density at high inlet gas relative humidity in polymer electrolyte membrane fuel cells. J Power Sources 422:163-174. https://doi.org/10.1016/j.jpowsour.2019.03.001

[30] Maizia R, Dib A, Thomas A, Martemianov S (2017) Proton exchange membrane fuel cell diagnosis by spectral characterization of the electrochemical noise. J Power Sources 342:553-561. https://doi.org/10.1016/j.jpowsour.2016.12.053

[31] Dib A, Maizia R, Martemianov S, Thomas A (2019) Statistical Short Time Analysis for Proton Exchange Membrane Fuel Cell Diagnostic-Application to Water Management. Fuel Cells 19:539-549. https://doi.org/10.1002/fuce.201900060

[32] Mortazavi M, Benner J, Santamaria A (2018) Evaluation of Liquid-Gas Two-Phase Flow Pressure Drop Signatures in Proton Exchange Membrane (PEM) Fuel Cell Flow Channels. ASME 2018 16th International Conference on Nanochannels, Microchannels, and Minichannels. https://doi.org/10.1115/icnmm2018-7667

[33] Mishima K, Hibiki T (1996) Some characteristics of air-water two-phase flow in small diameter vertical tubes. Int J Multiphase Flow 22:703-712. https://doi.org/10.1016/0301-9322(96)00010-9

[34] Xiao H, Mansfeld F (1994) Evaluation of coating degradation with electrochemical impedance spectroscopy and electrochemical noise analysis. J Electrochem Soc 141:2332. https://doi.org/10.1149/1.2055121

[35] Martemianov S, Adiutantov N, Evdokimov YK, Madier L, Maillard F, Thomas A (2015). New methodology of electrochemical noise analysis and applications for commercial Li-ion batteries. J Solid State Electrochem 19:2803-2810. https://doi.org/10.1007/s10008-015-2855-2

[36] Baert DHJ, Vervaet AAK (2003) Small bandwidth measurement of the noise voltage of batteries. J Power Sources 114:357-365. https://doi.org/10.1016/s0378-7753(02)00599-2

[37] Gabrielli C, Huet F, Keddam M (1986) Investigation of electrochemical processes by an electrochemical noise analysis. Theoretical and experimental aspects in potentiostatic regime. Electrochim Acta 31:1025-1039. https://doi.org/10.1016/0013-4686(86)80018-4

[38] Rubio MA, Bethune K, Urquia A, St-Pierre J (2016). Proton exchange membrane fuel cell failure mode early diagnosis with wavelet analysis of electrochemical noise. Int J Hydrogen Energy 41:14991-15001. https://doi.org/10.1016/j.ijhydene.2016.05.292

[39] Bertocci U, Frydman J, Gabrielli C, Huet F, Keddam M (1998) Analysis of electrochemical noise by power spectral density applied to corrosion studies: Maximum entropy method or fast Fourier transform?. J Electrochem Soc 145:2780. https://doi.org/10.1149/1.1838714

[40] Lee D, Bae J (2012) Visualization of flooding in a single cell and stacks by using a newly-designed transparent PEMFC. Int J Hydrogen Energy 37:422-435. https://doi.org/10.1016/j.ijhydene.2011.09.073

[41] Searson PC, Dawson JL (1988) Analysis of electrochemical noise generated by corroding electrodes under open-circuit conditions. Journal Electrochem Soc 135:1908. https://doi.org/10.1002/chin.198847019

[42] Mansfeld F, Lee CC (1997) The frequency dependence of noise resistance of polymer-coated metals. J Electrochem Soc 144:2062-2068 https://doi.org/10.1149/1.1837743

[43] Le AD, Zhou B, Shiu HR, Lee CI, Chang WC (2010) Numerical simulation and experimental validation of liquid water behaviors in a proton exchange membrane fuel cell cathode with serpentine channels. J Power Sources 195:7302-7315. https://doi.org/10.1016/j.jpowsour.2010.05.045

[44] Lee J, Hinebaugh J, Bazylak A (2013) Synchrotron X-ray radiographic investigations of liquid water transport behavior in a PEMFC with MPL-coated GDLs. J Power Sources 227:123-130. https://doi.org/10.1016/j.jpowsour.2012.11.006

[45] Lee S, Kim T, Park H (2011) Comparison of multi-inlet and serpentine channel design on water production of PEMFCs. Chem Engineering Science 66:1748-1758. https://doi.org/10.1016/j.ces.2011.01.007

[46] Aslam RM, Ingham DB, Ismail MS, Hughes KJ, Ma L, Pourkashanian M (2018) Simultaneous direct visualisation of liquid water in the cathode and anode serpentine flow channels of proton exchange membrane (PEM) fuel cells. J Energy Institute 91:1057-1070. https://doi.org/10.1016/j.joei.2017.07.003

[47] Choi KS, Kim HM, Moon SM (2011) Numerical studies on the geometrical characterization of serpentine flow-field for efficient PEMFC. Int J Hydrogen Energy 36:1613-1627. https://doi.org/10.1016/j.ijhydene.2010.10.073

[48] Kahveci EE, Taymaz I (2018) Assessment of single-serpentine PEM fuel cell model developed by computational fluid dynamics. Fuel 217:51-58. https://doi.org/10.1016/j.fuel.2017.12.073
[49] Shimpalee S, Lee WK, Van Zee JW, Naseri-Neshat H (2006) Predicting the transient response of a serpentine flow-field PEMFC: I. Excess to normal fuel and air. J Power Sources 156:355-368. https://doi.org/10.1016/j.jpowsour.2005.05.073
[50] Shimpalee S, Greenway S, Van Zee JW (2006) The impact of channel path length on PEMFC flow-field design. J Power Sources 160:398-406. https://doi.org/10.1016/j.jpowsour.2006.01.099
[51] Mansfeld F, Sun Z, Hsu CH (2001) Electrochemical noise analysis (ENA) for active and passive systems in chloride media. Electrochim Acta 46:3651-3664. https://doi.org/10.1016/s0013-4686(01)00643-0
[52] Lentka L, Smulko J (2019) Methods of trend removal in electrochemical noise data–Overview. Measurement 131:569-581. https://doi.org/10.1016/j.measurement.2018.08.023
[53] Maes K, Van Nimmen K, Gillijns S, Lombaert G (2017) Validation of time-delayed recursive force identification in structural dynamics. Procedia Engineering 199:2154-2159. https://doi.org/10.1016/j.proeng.2017.09.158
[54] Bahrami MJ, Shahidi M, Hosseini SMA (2014) Comparison of electrochemical current noise signals arising from symmetrical and asymmetrical electrodes made of Al alloys at different pH values using statistical and wavelet analysis. Part I: neutral and acidic solutions. Electrochim Acta 148:127–144. https://doi.org/10.1016/j.electacta.2014.10.031
[55] Xia DH, Behnamian Y (2015) Electrochemical noise: a review of experimental setup, instrumentation and DC removal. Russ J Electrochem 51(7):593–601. https://doi.org/10.1134/s1023193515070071
[56] Aballe A, Bethencourt M, Botana FJ, Marcos M (1999) Using wavelets transform in the analysis of electrochemical noise data. Electrochim Acta 44(26):4805–4816. https://doi.org/10.1016/s0013-4686(99)00222-4
[57] R Maizia, A Dib, A Thomas, S Martemianov (2018) Statistical short-time analysis of electrochemical noise generated within a proton exchange membrane fuel cell. J Solid State Electrochem 22:1649-1660. https://doi.org/10.1007/s10008-017-3848-0
[58] Dillet J, Lottin O, Maranzana G, Didierjean S, Conteau D, Bonnet C (2010) Direct observation of the two-phase flow in the air channel of a proton exchange membrane fuel cell and of the effects of a clogging/unclogging sequence on the current density distribution. J Power Sources 195:2795–2799. https://doi.org/10.1016/j.jpowsour.2009.10.103
[59] Lee D, Bae J (2012) Visualization of flooding in a single cell and stacks by using a newly-designed transparent PEMFC. Int J Hydrogen Energy 37:422-435. https://doi.org/10.1016/j.ijhydene.2011.09.073
[60] Iranzo A, Salva A, Boillat P, Biesdorf J, Tapia E, Rosa F (2017) Water build-up and evolution during the start-up of a PEMFC: Visualization by means of Neutron Imaging. Int J Hydrogen Energy 42:13839-13849. https://doi.org/10.1016/j.ijhydene.2016.11.076
[61] Legros B, Thivel PX, Bultel Y, Nogueira RP (2011) First results on PEMFC diagnosis by electrochemical noise. Electrochem Commun 13:1514–16. https://doi.org/10.1016/j.elecom.2011.10.007
[62] Astafev EA (2020) Comparison of Approaches in Electrochemical Noise Analysis Using an Air-Hydrogen Fuel Cell. Russian J Electrochem 56:156–162. https://doi.org/10.1134/s1023193520020032
[63] Astafev EA, Ukshe AE, Gerasimova EV, Dobrovolsky YA, Manzhos RA (2018) Electrochemical noise of a hydrogen-air polymer electrolyte fuel cell operating at different loads. J Solid State Electrochem 22:1839–1849. https://doi.org/10.1007/s10008-018-3892-4
[64] Martemianov S, Thomas A, Adiutantov N, Denisov E, Evdokimov Yu, Hissel D (2020) Electrochemical noise analysis of a PEM fuel cell stack under long-time operation: noise signature in the frequency domain. J Solid State Electrochem https://doi.org/10.1007/s10008-020-04759-z
[65] Wu Y, Cho JIS, Neville TP, Meyer Q, Ziesche R, Boillat P, Brett DJL (2018) Effect of serpentine flow-field design on the water management of polymer electrolyte fuel cells: an in-operando neutron radiography study. J Power Sources 399:254-263. https://doi.org/10.1016/j.jpowsour.2018.07.085
[66] Spernjak D, Prasad AK, Advani SG (2010) In situ comparison of water content and dynamics in parallel, single-serpentine, and interdigitated flow fields of polymer electrolyte membrane fuel cells. J Power Sources 195:3553-3568. https://doi.org/10.1016/j.jpowsour.2009.12.031
[67] Grimm M, See EJ, Kandlikar SG (2012) Modeling gas flow in PEMFC channels: Part I–Flow pattern transitions and pressure drop in a simulated ex situ channel with uniform water injection through the GDL. Int J Hydrogen Energy 37:12489-12503. https://doi.org/10.1016/j.ijhydene.2012.06.001